Neuroscience

The Journal of Physiology

JPn

Apelin acts in the subfornical organ to influence neuronal excitability and cardiovascular function

Li Dai, Pauline M. Smith, Markus Kuksis and Alastair V. Ferguson

Department of Biomedical & Molecular Sciences, Botterell Hall, 18 Stuart St., Room 435, Queen's University, Kingston, Ontario, K7L 3N6, Canada

Key points

- Apelin receptor mRNA is expressed in the subfornical organ.
- Apelin influences the excitability of the majority of subfornical organ neurons, with similar proportion showing depolarizing and hyperpolarizing effects.
- Hyperpolarizations appear to result from the activation of a sustained voltage-activated potassium conductance, while depolarizations may result from modulation of a non-selective cationic conductance.
- *In vivo* microinjection of apelin into the subfornical organ results in decreases in blood pressure.

Abstract Apelin is an adipocyte-derived hormone involved in the regulation of water balance, food intake and the cardiovascular system partially through actions in the CNS. The subfornical organ (SFO) is a circumventricular organ with identified roles in body fluid homeostasis, cardiovascular control and energy balance. The SFO lacks a normal blood–brain barrier, and is thus able to detect circulating signalling molecules such as angiotensin II and leptin. In this study, we investigated actions of apelin-13, the predominant apelin isoform in brain and circulatory system, on the excitability of dissociated SFO neurons using electrophysiological approaches, and determined the cardiovascular consequences of direct administration into the SFO of anaesthetized rats. Whole cell current clamp recording revealed that bath-applied 100 nM apelin-13 directly influences the excitability of the majority of SFO neurons by eliciting either depolarizing (31.8%, mean 7.0 ± 0.8 mV) or hyperpolarizing (28.6%, mean -10.4 ± 1.8 mV) responses. Using voltage-clamp techniques, we also identified modulatory actions of apelin-13 on specific ion channels, demonstrating that apelin-13 activates a non-selective cationic conductance to depolarize SFO neurons while activation of the delayed rectifier potassium conductance underlies hyperpolarizing effects. In anaesthetized rats, microinjection of apelin into SFO decreased both blood pressure (BP) (mean area under the curve -1492.3 ± 357.1 mmHg.s, $n = 5$) and heart rate (HR) (-32.4 ± 10.39 beats, $n = 5$). Our data suggest that circulating apelin can directly affect BP and HR as a consequence of the ability of this peptide to modulate the excitability of SFO neurons.

Introduction

Apelin, an adipocyte-derived hormone (Boucher *et al.* 2005), was initially isolated from bovine stomach extracts and finally identified as an endogenous ligand of the human orphan G-protein-coupled apelin receptor (APJ) (Tatemoto *et al.* 1998). Apelin is found in vascular endothelial cells and peripheral tissue, including heart, liver, kidney, lung and mammary glands (Habata *et al.* 1999;

O'Carroll *et al.* 2000; Kleinz & Davenport, 2004), and CNS (Hosoya *et al.* 2000; O'Carroll *et al.* 2000; Kawamata *et al.* 2001; Reaux *et al.* 2001; Medhurst *et al.* 2003). This peptide is derived from a 77 amino acid precursor and then undergoes post-translational processing into a number of different forms, including apelin-36, apelin-17 and apelin-13, all of which share the fully conserved C-terminal sequence (Tatemoto *et al.* 1998). These products all have high affinity for APJ and similar biological properties, such as promoting the extracellular acidification, suppressing forskolin-stimulated cAMP production, and inducing APJ internalization (Tatemoto *et al.* 1998; Zou *et al.* 2000; Medhurst *et al.* 2003; El Messari *et al.* 2004; Iturrioz *et al.* 2010). Apelin-13 is the predominant molecular form of endogenous apelin in brain and plasma (De Mota *et al.* 2004; Azizi *et al.* 2008) and exhibits clear biological activity and affinity for the APJ receptor (Tatemoto *et al.* 1998).

Apelin, through actions at the APJ receptor, has been shown to influence a variety of physiological systems, including fluid homeostasis (Lee *et al.* 2000; Taheri *et al.* 2002; De Mota *et al.* 2004; Roberts *et al.* 2009), metabolic control (Taheri *et al.* 2002; Sunter *et al.* 2003; Boucher *et al.* 2005; Wei *et al.* 2005; Valle *et al.* 2008; Lv *et al.* 2011) the immune response (Cayabyab *et al.* 2000; Horiuchi *et al.* 2003) and cardiovascular function (Tatemoto *et al.* 2001; Lee *et al.* 2005). Interestingly, while intravenous injection of apelin causes drinking and decreases in blood pressure (BP) in rats (Lee *et al.* 2000; Tatemoto *et al.* 2001; Cheng *et al.* 2003), central (intracerebroventricular, I.C.V.) administration of this peptide has either no effect on cardiovascular function (Reaux *et al.* 2001) or increases mean arterial pressure and heart rate (HR, Seyedabadi *et al.* 2002; Kagiyama *et al.* 2005), suggesting a divergence of peripheral and central actions of apelin. The subfornical organ (SFO), one of the circumventricular organs (CVOs) of the brain (structures lacking a normal blood–brain barrier), has been identified as a potential site at which circulating signals involved in the regulation of cardio-vascular and metabolic function may influence the brain (Mangiapane & Simpson, 1980*a*; Smith & Ferguson, 1997; Riediger *et al.* 1999; Smith & Ferguson, 2012). Adiponectin, amylin, angiotensin II, leptin, vasopressin, orexin-A and relaxin have all been shown to influence central autonomic pathways by modulating the neuronal activity of individual SFO neurons (Anthes *et al.* 1997; Ferguson *et al.* 1997; Riediger *et al.* 1999; Ono *et al.* 2008; Smith *et al.* 2009; Alim *et al.* 2010) through efferent projections of SFO neurons to hypothalamic autonomic control centres including the arcuate, medial preoptic and paraventricular nuclei (PVN) (Gruber *et al.* 1987; Lind *et al.* 1982). In addition, direct administration of many of these signalling molecules into the SFO has been shown to influence cardiovascular function (Mangiapane & Simpson, 1980*b*; Smith & Ferguson, 1997; Smith *et al.*

2007). Destruction of the SFO has also been shown to abolish both the pressor response and drinking induced by intravenous injection of angiotensin II (Mangiapane & Simpson, 1980*a*; Collister & Nahey, 2009), highlighting the critical role for this CVO in transmitting sensory information carried by these circulating signals to central control centres protected by the normal blood–brain barrier.

Apelinergic fibres innervating the SFO have been reported (Reaux *et al.* 2002), while our microarray analysis of the transcriptome of the SFO demonstrated mRNA for the APJ receptor in this CVO (Hindmarch *et al.* 2008). These observations suggest a functional role for the SFO in monitoring both neurally derived and/or circulating apelin, and this study was therefore undertaken to investigate the physiological and cellular actions of apelin actions in the SFO.

Methods

All experiments and animal protocols conformed to the standards of the Canadian Council on Animal Care and were approved by the Queen's University Animal Care Committee.

SFO neuron preparation

SFO neurons were prepared from brains removed rapidly from male Sprague-Dawley rats (100–150 g) following decapitation. Tissue was placed in ice-cold oxygenated artificial cerebrospinal fluid (aCSF) containing: 124 mM NaCl, 2.5 mM KCl, 1.24 mM KH_2PO_4, 2.27 mM $CaCl_2$, 1.3 mM $MgSO_4$, 20 mM $NaHCO_3$ and 10 mM glucose. Under a dissecting microscope, the SFO was identified and removed from the ventral surface of the fornix and transferred into Hibernate medium (Brain Bits, Springfield, IL, USA) containing 2 mg ml^{-1} papain (Worthington Biochemical, Lakewood, NJ, USA). After 30 min incubation at 31°C, the SFO was rinsed three times, gently triturated with Hibernate medium supplemented with B27 (Life Technologies Inc., Carlsbad, CA, USA), and dissociated neurons were collected in a pellet by centrifugation at 200 g for 5 min at 4°C. The cells were resuspended in B27 supplemented Neurobasal A medium (Life Technologies) containing 100 U ml^{-1} penicillin-streptomycin, 0.5 mM L-glutamine (Life Technologies) and 5 mM glucose, and aliquoted to 35 mm glass-bottomed culture dishes (MatTek, Ashland, MA, USA). The cells were maintained in the incubator at 37°C in 5% CO_2. After the neurons adhered to the bottom of the culture dish (approximately 3 h) additional B27 supplemented Neurobasal A was added. These techniques as well as viability of dissociated neurons have been described in depth previously (Ferguson *et al.* 1997).

RT-PCR

Total RNA was extracted from acutely microdissected SFO tissue using an RNAqueous-Micro kit (Ambion, Austin, TX, USA). After DNase treatment, the total RNA was transcribed to cDNA using a Superscript III first strand synthesis kit (Life Technologies). RT-PCR was carried out with a Qiagen multiplex PCR kit (Qiagen, Valencia, CA, USA) using primers specific for rat APJ (NM_031349.2 forward primer: 5′-TTCCTTCTAGGCACCACAGG-3′; reverse primer: 5′-CCAAAAGGCCAGTCAAACTC-3′, yielding a 179 bp product). The reaction was denatured at 95°C for 15 min and cycled 30 times through a temperature protocol consisting of 20 s at 94°C, 30 s at 60°C and 40 s at 72°C. PCR products were analysed on a 1.5% agarose gel.

Electrophysiology

Voltage and current clamp recordings were obtained from SFO neurons 1–4 days after dissociation using a Multiclamp 700B patch-clamp amplifier (Molecular Devices, Sunnyvale, CA, USA). Recording and stimulation were carried out using Signal (version 4) and Spike2 (version 6) software (Cambridge Electronics Design, Cambridge, UK). Membrane potential and whole-cell current data were digitized at 5 kHz and filtered at 1 kHz using a Cambridge Electronics Design Micro1401 interface. Patch-clamp recording in the whole-cell mode was performed using the perforated patch method as previously described (Price *et al.* 1999). Electrodes were fabricated from borosilicate glass (World Precision Instruments, Sarasota, FL, USA) and fire-polished. When filled with internal solution containing 55 mM KCl, 75 mM potassium acetate, 8 mM $MgCl_2$ and 10 mM Hepes (pH 7.3 with KOH), electrodes had a resistance of 2–4 MΩ. The external recording solution contained 140 mM NaCl, 5 mM KCl, 1 mM $MgCl_2$, 2 mM $CaCl_2$, 10 mM Hepes, 5 mM mannitol and 5 mM glucose, and pH was adjusted to 7.3 with NaOH.

Dissociated SFO neurons were perfused with external recording solution (32°C) at a rate of 1.6 ml min^{-1}. Once whole cell configuration was achieved, cells were defined as neurons by the presence of voltage-gated Na$^+$ currents under voltage-clamp configuration and the occurrence of spontaneous or current evoked action potentials (amplitude greater than 50 mV) in current clamp configuration. A calculated junction potential of −14.4 mV was added to the membrane potential of recorded neurons. After a minimum 200 s stable baseline membrane potential was established, various concentrations (from 1 fM to 100 nM) of apelin-13 (Phoenix Pharmaceuticals) was applied followed by a wash with external recording solution. Responsiveness of SFO neurons was determined by comparing membrane potential of neurons before and after apelin-13 application. Membrane potential changes were determined by comparing the average membrane potential during the 100 s control period, with sequential 100 s periods after apelin-13 application. SFO neurons were considered responsive to apelin-13 application if the difference in membrane potential was greater than twice the standard deviation of the control baseline membrane potential and the cell showed a partial recovery toward baseline values following removal of the apelin-13 from the bath. Reported changes in membrane potential represent the 100 s mean with the largest change from the control period.

In voltage-clamp experiments, currents were recorded using a slow voltage ramp protocol (12 mV s^{-1}, from −100 to 0 mV), prior to and after administration of apelin-13 in bath solution to assess the effects of bath-applied apelin-13 on whole cell currents. SFO neurons were clamped at −80 mV, and ramp currents were determined from an average of three ramps. The apelin-13-induced difference current was calculated by subtraction of the control current before administration of apelin-13 from the current obtained after peptide treatment. Linear regression analysis was used to determine reversal potential. Full current–voltage (*I*–*V*) relationships were evaluated using voltage step protocols before and after apelin-13 application. Whole cell currents were evoked by voltage steps from −120 to 10 mV in 10 mV increments from a holding potential of −80 mV and the *I*–*V* relationship was constructed using the average current recorded during the final 10 ms of each voltage step plotted against the corresponding voltage.

Mean change (± SEM) in membrane potential or currents before and after apelin-13 administration were calculated as described above, and changes were compared using a Student's *t* test. All statistical analyses were performed using GraphPad Prism (version 5.0).

Microinjection

Urethane-anaesthetized (1.4 g kg^{-1}) male Sprague-Dawley rats (150–350 g) were placed on a feedback-controlled heating blanket for the duration of the experiment to maintain body temperature at 37°C. Urethane was elected for use in these studies in association with its ability to maintain long lasting stable levels of anaesthesia. Animals were fitted with an indwelling femoral arterial catheter (Intramedic PE50 Tubing) for the measurement of BP and HR. The animal was then placed in a stereotaxic frame and a midline incision was made through the skin of the skull. A small burr hole was drilled in the skull such that a microinjection cannula (150 μm tip diameter; Rhodes Medical Instruments, Summerland, CA, USA) could be advanced into the region of the

SFO according to the coordinates of Paxinos & Watson (1982; Bregma −0.8 mm, ventral 4.5 mm, midline). After a minimum 2 min stable baseline recording was obtained, apelin-13 (0.5 μl of 10^{-7} M-50 fmol, dissolved in aCSF) or aCSF (0.5 μl, vehicle control) was microinjected into the region by a pressure-driven 10 μl Hamilton micro-syringe over 10 s and the effects on BP and HR were assessed. At the conclusion of the experiment, animals were overdosed with anaesthetic, perfused through the left ventricle of the heart with 0.9% saline followed by 10% formalin, and the brain removed and placed in formalin for at least 24 h. Coronal sections (100 μm) were cut through the region of the SFO using a vibratome, mounted and stained with cresyl violet. The anatomical location of microinjection sites were verified at the light microscope level by an observer unaware of the experimental protocol or the data obtained.

Animals were assigned to one of two anatomical groups (SFO or non-SFO) according to the location of the micro-injection site. Animals with injection sites that were not wholly confined within either of these regions were excluded from further analysis. Animals with confirmed microinjection sites in the SFO were further divided according to whether apelin-13 (50 fmol) or aCSF (vehicle control) was microinjected into the region. Normalized BP and HR data (mean baseline BP and HR data were calculated for 60 s before injection and subtracted from all data points before and after injection) were obtained for each animal 60 s before the time of microinjection (control period) until 200 s after microinjection. The area under the curve (AUC, area between baseline and each BP and HR response) was calculated for each animal for the 200 s immediately following the injection. Mean AUC for BP and HR responses for each group were then calculated. A one-way analysis of variance (one-way ANOVA, followed by Newman-Keuls *post hoc* analysis) was used to determine whether BP and HR responses observed in response to substance administered (apelin-13 or aCSF) into the SFO or anatomical location of apelin-13 administration (SFO or non-SFO) were statistically significant.

Chemicals

All chemicals were purchased from Sigma (St Louis, MO, USA), unless otherwise specified.

Results

Apelin influences the excitability of SFO neurons

Using RT-PCR, we detected expression of the apelin receptor gene, APJ, in SFO tissue (Fig. 1), and then utilized whole-cell recording techniques to access the effects of

bath administration of apelin-13 on membrane potential of SFO neurons. We obtained recordings from 171 SFO neurons with resting membrane potentials between −46 and −62 mV, input resistance between 3.02 and 0.64 GΩ, spike amplitudes between 65 and 85 mV, and spontaneous activity (observed in 51% of recorded neurons) with a mean frequency of 2.41 ± 0.24 Hz. These data are in accordance with our previous recordings from SFO neurons (Ferguson *et al.* 1997; Desson & Ferguson, 2003).

We first examined the sensitivity of SFO neurons to bath application of 100 nM apelin-13 ($n = 63$) which, as illustrated in Fig. 2, significantly changed membrane potential in 60.3% ($n = 38$) of SFO neurons tested, with approximately equal proportions of apelin-13-sensitive neurons showing depolarizations (31.8%, mean $= 7.0 \pm 0.80$ mV, $n = 20$; Fig. 2A) or hyperpolarizations (28.6%, mean $= -10.4 \pm 1.8$ mV, $n = 18$; Fig. 2B). Depolarizing responses showed relatively quick onsets (<250 s), were accompanied by increased spike frequency, as illustrated in Fig. 2A, and often lasted up to 15 min before return to baseline. Apelin-13-induced hyperpolarizations usually occurred within 180 s and were often accompanied by a reduced spontaneous action potential frequency (see Fig. 2B). The remaining 39.7% ($n = 25$) of tested SFO neurons did not exhibit any significant changes in membrane potential (0.1 ± 0.32 mV, $n = 25$, Fig. 2C) or spike frequency (-0.09 ± 0.232 mV, $n = 25$, Fig. 2D) in response to bath administration of apelin-13, suggesting the existence of subpopulations of SFO neurons with differential sensitivity to apelin-13. Importantly, bath administration of 500 nM apelin F13A (an apelin receptor antagonist) inhibited single cell responses to 100 nM apelin-13 as only 1 of 10 cells tested responded (with a small depolarization $+5.3$ mV). The chi-squared test showed that effects
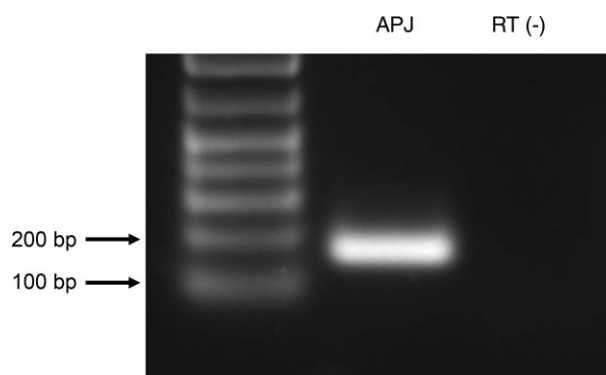

Figure 1. Agarose gel RT-PCR analysis of SFO cDNA for APJ gene expression
The PCR product (179 bp) for APJ is clearly present in SFO tissue but absent in the RT(−) reaction in which reverse transcriptase has been omitted from the cDNA synthesis reaction.

after F13A were significantly different from the normal depolarizing and hyperpolarizing effects of apelin-13 ($P < 0.005$).

Interestingly, the magnitude of the changes in membrane potential of SFO neurons in response to apelin-13 did not show a typical concentration–response relationship, as depolarizations (between 5.4 ± 1.4 and 7.0 ± 0.8 mV) or hyperpolarizations (between -6.5 ± 1.5 and 9.8 ± 1.4 mV) were similar when 1 pM ($n = 13$), 1 nM ($n = 28$), 10 nM ($n = 26$) or 100 nM ($n = 63$) apelin-13 was administrated. In addition, the percentage of neurons influenced by apelin-13 was similar at all effective concentrations (between 47.8 and 60.3%). Statistical analysis of these parameters showed that neither the amplitude of membrane potential nor the proportion of responsive cells showed significant differences in response to apelin-13 at concentrations between 1 pM and 100 nM ($P > 0.05$, one-way ANOVA), suggesting that the maximal response is in fact observed at 1 pM. This observation is in accordance with previous studies showing that the total concentration of circulating apelin (mainly apelin-17 and apelin-13) in rat plasma is around 3.4 ± 0.25 pM (De Mota *et al.* 2004). We therefore reduced the concentration of apelin-13 applied to 100 fM and, of 16 SFO neurons tested, one-third responded with three cells showing depolarization (7.5 ± 0.7 mV) and two displaying hyperpolarization (-7.9 ± 0.2 mV). A further reduction to 1 fM apelin-13 resulted in 2 of 13 cells tested responding, one showing depolarization ($+8.2$ mV) and the other a hyperpolarization (-7.7 mV). Although the amplitudes of changes in membrane potential did not show any obvious reduction at these lower concentrations, the percentage of responding neurons was reduced to 31% (100 fM) and 15% (1 fM). The average absolute value of any change in membrane potential for all SFO neurons tested with each concentration, including non-responsive cells, can be calculated and thus provide a mean absolute change in membrane potential for 100 nM (5.2 ± 0.5 mV),
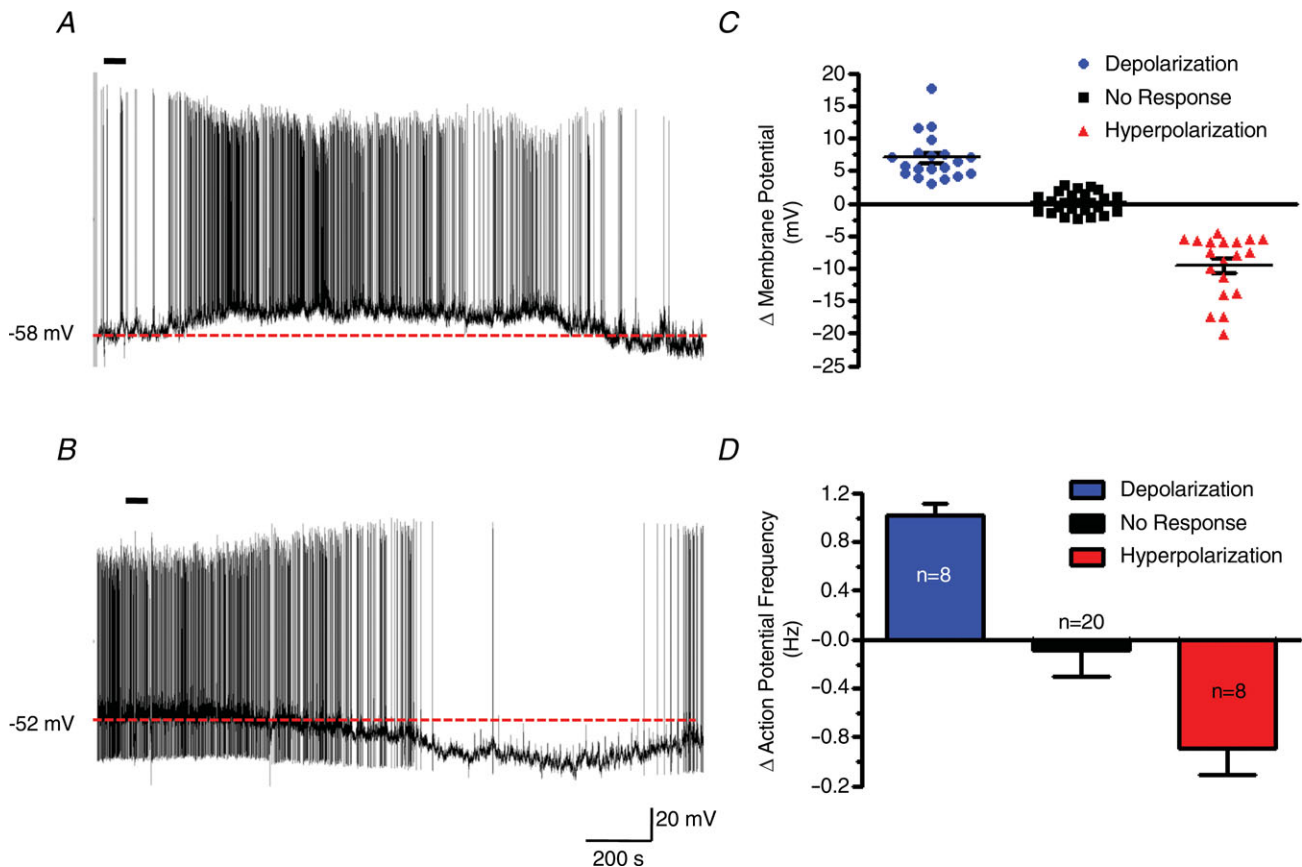
Figure 2. Current-clamp recordings and changes in membrane potential and action potential frequency for cells treated with apelin-13
*A* and *B*, representative current-clamp recordings from neurons that depolarized (*A*) or hyperpolarized (*B*) in response to bath application of 100 nM apelin-13 (black bar). *C* and *D*, graphs representing mean changes in membrane potential (*C*) and action potential frequency (*D*) for cells treated with 100 nM apelin-13. SFO neurons in which sodium channels inactivated after depolarization and neurons that were quiescent before hyperpolarization were not included in the analysis of the mean change in action potential frequency. Each bar represents the mean ± SEM for group data.

1 pM (4.6 ± 1.0 mV), 100 fM (3.2 ± 0.8 mV) and 1 fM (2.0 ± 0.8 mV), as illustrated in Fig. 3.

Apelin-13 modulates a K^+ conductance and a non-selective cationic conductance in SFO neurons

We next undertook experiments designed to investigate the potential ion channels underlying the differential depolarizing and hyperpolarizing effects of apelin-13 on SFO neurons. These studies were carried using a recording protocol in which we first obtained voltage clamp recordings to assess whole cell currents in response to slow voltage ramps (-100 to 0 mV, 12 mV s^{-1}) and standard depolarizing pulse protocols (-120 to 10 mV from holding potential of -80 mV in 10 mV increments) under control conditions. Recording configuration was then changed to current clamp and 100 nM apelin-13 was administered, as described above, and initial effects on membrane potential assessed such that the cell could be classified as depolarized, hyperpolarized or unaffected by apelin-13. The recording configuration was then switched back to voltage clamp and the currents in response to slow voltage ramps and step protocols were reassessed such that changes, and thus the apelin-13-evoked current, could be determined by subtraction.

Voltage ramp analysis of 14 SFO neurons which hyperpolarized in response to apelin-13 (see Fig. 4*Aa*) show a linear apelin-13-induced whole cell current ($r^2 = 0.97$) within the voltage range of -100 to -40 mV with a mean reversal potential of -78.6 ± 3.2 mV (Fig. 4*Ab*), suggesting the involvement of a potassium conductance in mediating the hyperpolarizing response to apelin-13. In addition, these voltage ramps showed that apelin-13
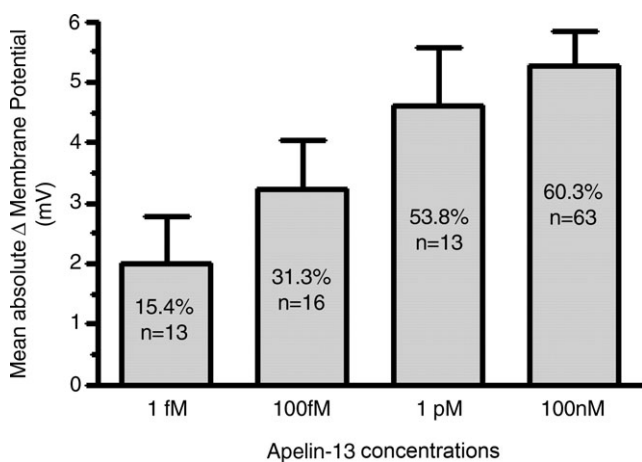
Figure 3. Absolute changes in membrane potential of SFO neurons in response to increasing concentrations of apelin-13
Mean (±SEM) absolute changes in the membrane potential of SFO neurons in response to increasing concentrations (1 fM to 100 nM) of apelin-13. The percentage of apelin-13-responsive SFO neurons and *n* values are indicated in columns.

induced a large voltage-dependent outward current which activated at approximately -30 mV (see Fig. 4*Ab*), currents which suggested effects on voltage-activated sustained K^+ current (I_K). Analysis of voltage clamp pulse protocols in the 14 hyperpolarized SFO neurons identified a considerable increase in amplitude of sustained K^+ current in response to voltage steps to 0 mV from a mean of 0.68 ± 0.08 nA in control conditions to 0.87 ± 0.11 nA during apelin-induced hyperpolarization, effects that show a statistically significant increase in current (paired 't' test $P < 0.05$ $n = 14$). These changes represent a normalized increase in current at steps to both 0 mV ($25.7 \pm 9.9\%$) and 10 mV ($17.8 \pm 7.7\%$), as illustrated in Fig. 5. In contrast, SFO neurons that depolarized in response to apelin-13 showed no such effects on amplitude of sustained K^+ current in response to the same voltage steps (0 mV $2.5 \pm 7.3\%$; 10 mV $5.4 \pm 6.8\%$, $n = 7$). Interestingly, unlike the increased sustained K^+ current, the peak value of transient K^+ (putative but uncharacterized I_A) from hyperpolarized SFO neurons was reduced (0 mV $-16.1 \pm 4.5\%$, $n = 14$), but was unaffected in SFO neurons depolarized by apelin-13 (0 mV $+0.7 \pm 3.0\%$, $n = 7$) as illustrated in Fig. 5 and summarized in Fig. 5*C*.

We next used 30 mM tetraethylammonium to block I_K and determine whether the apelin-13-induced hyperpolarization was still observed in SFO neurons. We tested 10 neurons in tetraethylammonium, of which 3 showed no response to apelin-13 (-0.08 ± 1.17 mV), 5 depolarized (7.96 ± 1.46 mV), and two responded with small (-2.63 and -3.37 mV) hyperpolarizations that were clearly smaller than the mean hyperpolarizing effects observed in aCSF (-10.4 ± 1.8 mV). In contrast, linear regression analysis for the I–V curve of apelin-13-induced currents from depolarized SFO neurons (data were collected successfully from four depolarized cells) revealed that the net apelin-13-induced whole cell current displayed a linear relationship between -100 and -30 mV ($r^2 = 0.96$, see Fig. 4*Ba*), with a mean reversal potential of -25.9 ± 5.3 mV ($n = 4$) (Fig. 4*Bb* inset), characteristic of a non-selective cationic conductance (NSCC) (Oliet & Bourque, 1993; Desson & Ferguson, 2003; Pulman *et al.* 2006).

Apelin microinjection into the SFO decreases BP and HR

Twenty animals were used in this study, 10 of which had microinjection locations entirely within the SFO (SFO group – baseline BP: 84.97 ± 6.8 mmHg, HR: 417.20 ± 19.9 b.p.m.) while 4 had microinjection locations wholly outside the SFO (non-SFO – baseline BP: 89.34 ± 5.0 mmHg, HR: 440.37 ± 6.3 b.p.m., values which were not significantly different from the SFO group). The remaining animals ($n = 6$) were excluded from further

analysis as sites could not be reliably classified as either SFO or non-SFO sites.

Microinjection of apelin-13 (50 fmol) into the SFO resulted in rapid, long lasting (>5 min) decreases in BP (mean AUC $= -1492.3 \pm 357.1$ mmHg∗s, $n = 5$, $P < 0.01$ Newman Keuls *post hoc* analysis *vs.* non-SFO and aCSF; see Fig. 6A) and HR (mean AUC $= -32.4 \pm 10.4$ beats, $n = 5$; $P < 0.05$ Newman–Keuls *post hoc* analysis *vs.* non-SFO and aCSF; see Fig. 6B). Apelin-13 microinjection elicited a significant ($P < 0.05$, one-way ANOVA) maximal decrease in BP (mean $= -9.7 \pm 3.5$ mmHg, $n = 5$) and HR (mean $= -14.2 \pm 5.4$ b.p.m.) which occurred within 2 min of apelin-13 administration. These effects were due to the administration of apelin-13, as microinjection of aCSF (vehicle) was without effect on BP (mean AUC $= -64.2 \pm 166.6$ mmHg∗s, $n = 5$) or HR (mean AUC $= 0.78 \pm 3.3$ beats, $n = 5$). In addition, BP effects were shown to be site specific, as apelin-13 microinjection into non-SFO regions was without effect on BP (mean

AUC $= -276.2 \pm 131.3$ mmHg∗s, $n = 4$) or HR (mean AUC $= 2.6 \pm 5.4$ beats, $n = 4$).

Discussion

The present study provides the first evidence supporting a functional role for the SFO as a CNS target through which apelin may act to influence both cardiovascular, metabolic and body fluid regulation. Our patch clamp recordings demonstrate that apelin-13 directly modulates the excitability of the majority of dissociated SFO cells and thus suggests that these neurons represent a potential site in the CNS at which either centrally produced or circulating apelin may act to influence central autonomic pathways without crossing the blood–brain barrier. These observations are in accordance with studies showing c-Fos expression in SFO neurons in response to intra-peritoneal administration of apelin (Takayama *et al.* 2008), although it should be emphasized that such observations are not in accordance with hyperpolarizing
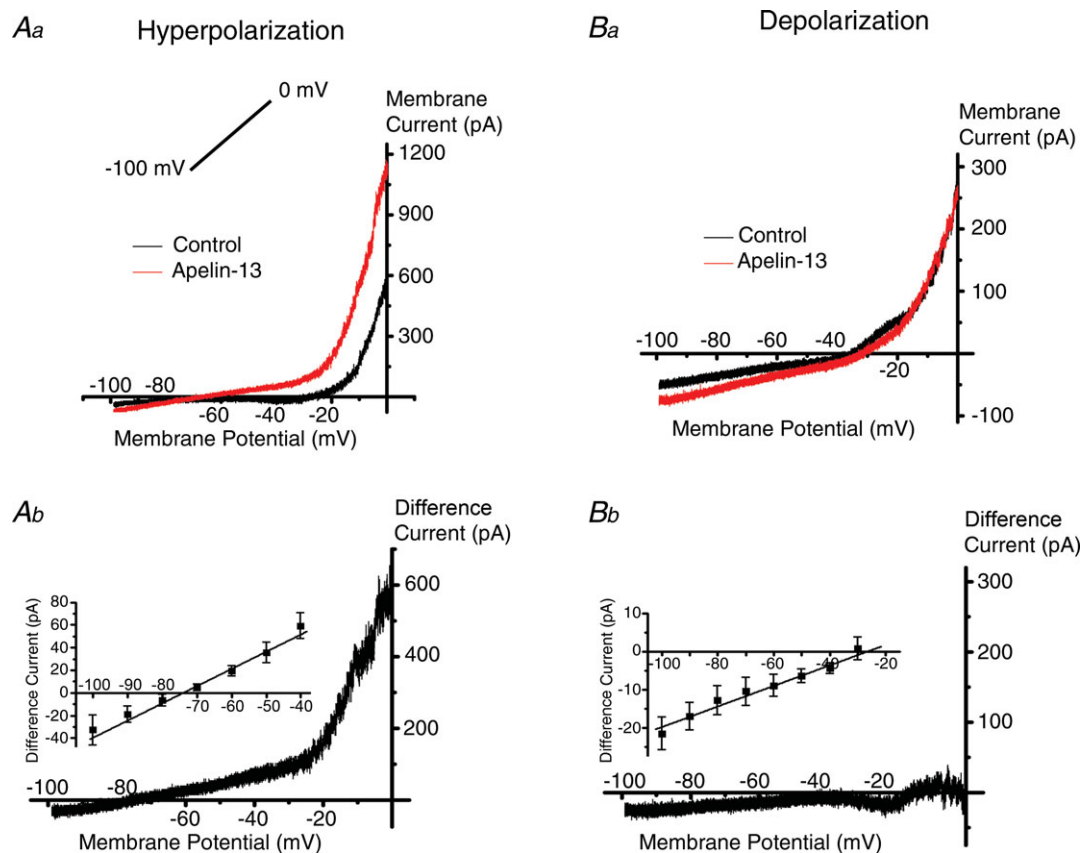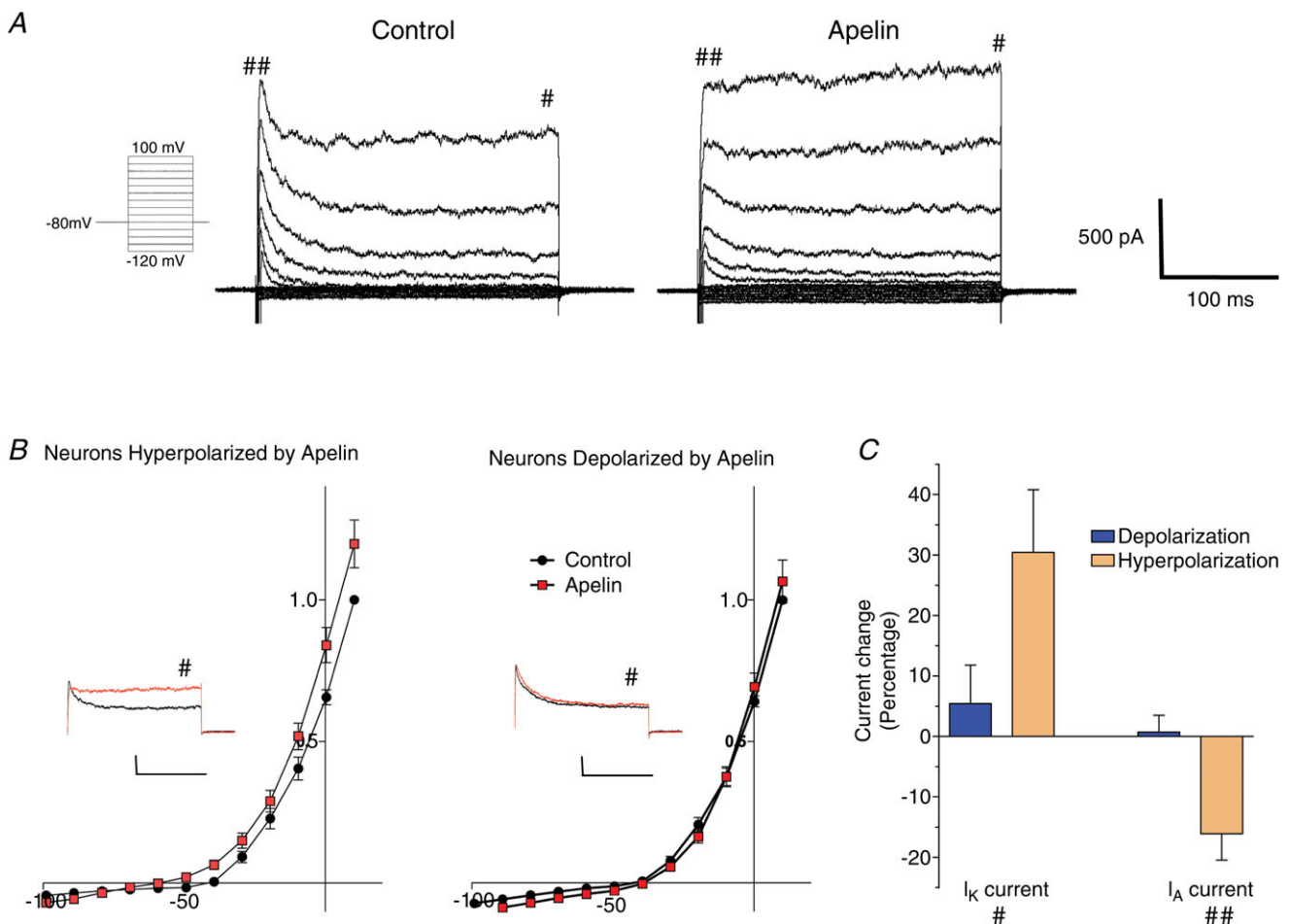

Figure 4. Currents recorded from SFO neurons in response to slow voltage ramps before and during apelin-13-induced hyperpolarization or depolarization
Representative traces of currents recorded from SFO neurons in response to slow voltage ramps (12 mV s^{-1}: *Aa* inset) before (black traces) and during (red traces) apelin-13-induced hyperpolarization (*Aa*) or depolarization (*Ba*). The lower traces shown in *Ab* and *Bb* show the net apelin-13-induced (difference) current elicited, which is derived by subtracting control currents (black) from apelin-13-affected current (red) which are recorded from the same neurons as shown in upper panels. The insets in *Ab* and *Bb* show the mean *I–V* curves (±SEM) of net apelin-13-induced current in hyperpolarized (*Ab*, $n = 14$) and depolarized (*Bb*, $n = 4$) neurons.

actions. Our recordings do, however, suggest the presence of different subpopulations of SFO neurons which depolarize, hyperpolarize or are unaffected by apelin, observations which are in accordance with previous studies evaluating adiponectin and leptin actions on SFO neurons (Smith *et al.* 2009; Alim *et al.* 2010). The functional relevance of these different groups of SFO neurons is not fully understood but may be related to roles either within the SFO (projection *vs.* interneurons) or to the specific efferent projections (PVN projecting *vs.* arcuate projecting) of single SFO neurons.

Our voltage clamp recordings in which we measured currents in response to slow voltage ramps in SFO neurons depolarized by apelin-13 revealed an apelin-induced current which was voltage independent and exhibited a reversal potential near −25 mV, indicating that such effects probably result from the activation of an NSCC. These observations are in accordance with a previous study showing that apelin depolarizes hypothalamic magnocellular vasopressin neurons through similar activation of a putative NSCC with reversal potential of -32 ± 2 mV (Tobin *et al.* 2008). Interestingly, other circulating hormones including angiotensin II (Ono *et al.* 2001; Washburn & Ferguson, 2001), ghrelin (Pulman *et al.* 2006) and interleukin 1β (Desson & Ferguson, 2003) have all been shown to influence the excitability of SFO neurons through the modulation of this conductance, which has also been suggested to be a critical site for integration in supraoptic magnocellular neurons (Hiruma & Bourque, 1995).

**Figure 5. Apelin-13 increases I$_K$ in SFO neurons hyperpolarized by this peptide.**
A, whole cell K$^+$ currents recorded from an SFO neuron hyperpolarized by apelin-13 in response to voltage steps protocol (inset) before peptide application (left) and during apelin-13-induced hyperpolarization (right). *B*, mean *I–V* curves showing currents measured at the end of voltage pulses (# – sustained current) in neurons which were hyperpolarized ($n = 14$ – left panel) or depolarized ($n = 7$ – right panel) by apelin-13 (black activation curves are control and red indicate *I–V* curves during apelin-13). The insets show overlaid traces recorded at 0 mV from control (black trace), hyperpolarized or depolarized neurons (red trace). *C*, bar graph showing the summary (mean ± SEM) changes in normalized amplitudes of the sustained K$^+$ (*I$_K$*) and transient K$^+$ (*I$_A$* – peak current measured in the first 50 ms of pulse ##) elicited at the 0 mV voltage step from SFO neurons in which apelin-13 induced depolarization ($n = 7$, blue bar) and hyperpolarization ($n = 14$, orange bar).

In contrast to the supraoptic nucleus where administration of apelin induced only depolarizations (Tobin *et al.* 2008), nearly 30% of SFO neurons were hyperpolarized by 100 nM apelin-13. In these hyperpolarized neurons, currents recorded in response to voltage ramps (-100 and -20 mV) revealed an apelin-induced voltage-independent outward current with a reversal potential of -75 mV, suggesting effects on a potassium channel. At voltages positive to -20 mV, the slope of the difference current increased abruptly, indicating the additional involvement of a voltage-gated conductance. These observations led us to examine currents evoked by standard voltage step protocols, which confirmed apelin activation of the sustained potassium current, I_K. These data therefore suggest that multiple potassium channels may contribute to apelin-mediated hyperpolarization of

SFO neurons as has previously been shown for other neuropeptide actions in SFO, arcuate nucleus, PVN, area postrema and nucleus tractus solitarius (Yang & Ferguson, 2003; Fry & Ferguson, 2009; Hoyda & Ferguson, 2010).

The functional relevance of different apelin effects of these subpopulations of SFO neurons remains to be determined. Through extensive efferent projections to hypothalamic autonomic control and neuroendocrine centres, the SFO participates in the regulation of fluid balance, energy homeostasis and cardiovascular control. The heterogeneity of apelin effects on SFO neurons could reflect the association between these subpopulations and their specific connections to different hypothalamic nuclei (e.g. PVN *vs.* arcuate projecting) where the afferent information will be integrated to determine the final physiological effects.
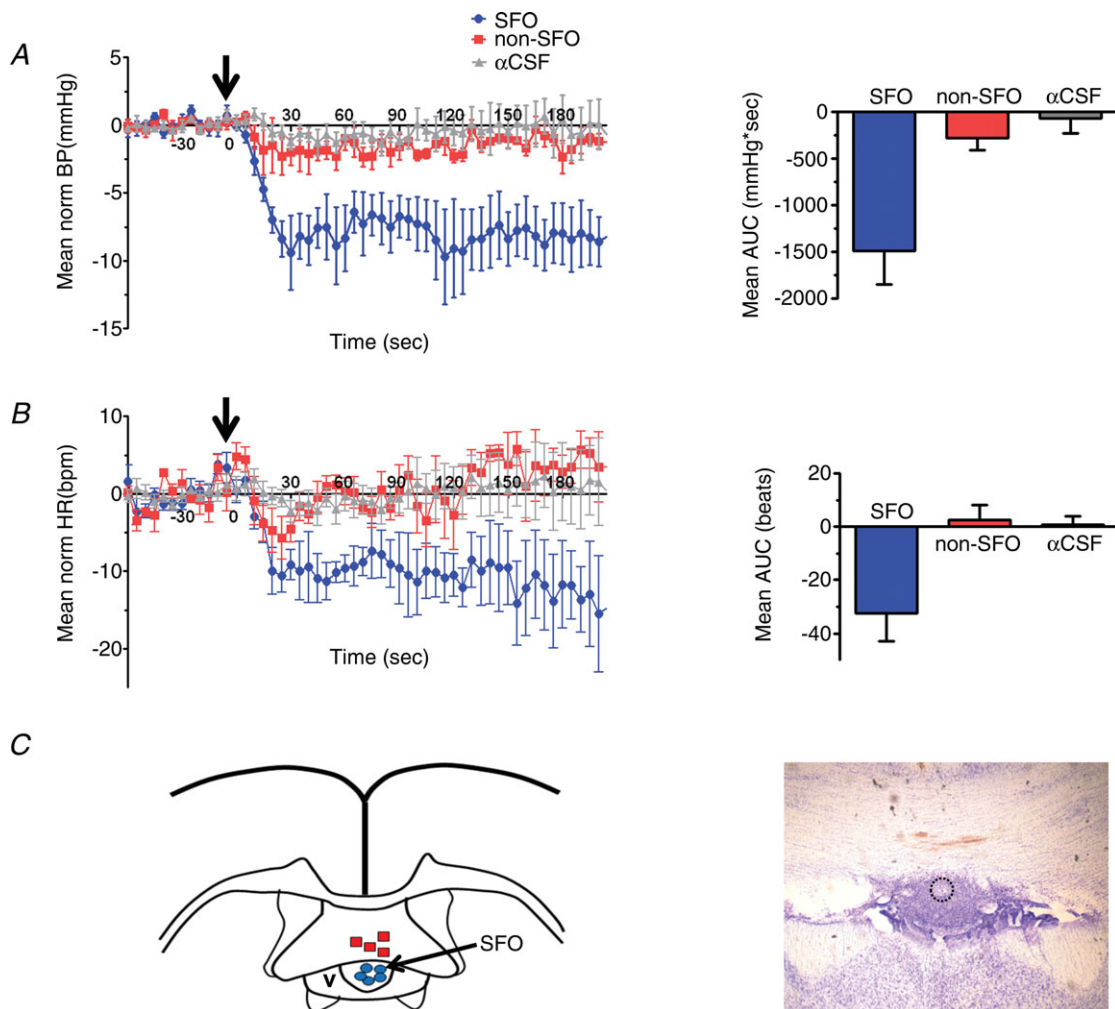
Figure 6. Apelin-13 acts in SFO to decrease blood pressure and heart rate.
A and *B*, normalized mean BP (*A*, left) and HR (*B*, left) traces in response to a bolus (0.5 μl) microinjection (time indicated by the arrow) of apelin-13 (50 fmol – blue) or vehicle control (aCSF – grey) into the SFO or apelin-13 into non-SFO (red) locations. The bar graphs on the right show mean AUC for BP and HR. *C*, the schematic diagram on the left illustrates SFO (blue circles) and non-SFO (red squares) microinjection locations while the photomicrograph to the right shows the anatomical location of an SFO microinjection site (within the circle) in a 100 μm cresyl violet-stained coronal section.

The effects of apelin on cardiovascular function have been widely studied with the consensus being that intravenous apelin decreases BP in both anaesthetized and conscious rats (Tatemoto *et al.* 2001; Cheng *et al.* 2003; El Messari *et al.* 2004), although effects on HR are more variable. In association with such observations, our microinjection studies showed that direct administration of very low doses (50 fmol) also caused rapid decreases in BP and HR. The fact that BP and HR were influenced in the same manner, i.e. both were decreased by apelin-13 administration, indicates that these responses represent a regulated decrease in BP as no baroreflex-mediated increase in HR was observed. Importantly, these effects were site specific (not observed in non-SFO sites) and not a result of mechanical changes in tissue (vehicle controls were without effect), suggesting specific cardiovascular actions of apelin within the SFO. These effects are consistent with the depressor effects observed in response to peripheral administration of low doses of apelin (Lee *et al.* 2000; Tatemoto *et al.* 2001; Cheng *et al.* 2003) but are in contrast to pressor responses following peripheral administration of higher doses (Kagiyama *et al.* 2005). Pressor effects to both I.C.V. (Kagiyama *et al.* 2005) or site-specific microinjections of apelin into nucleus tractus solitarius or rostral ventral lateral medulla (Seyedabadi *et al.* 2002) suggest differential functional roles for hormonal (depressor) *vs.* neurotransmitter (pressor) apelin, and perhaps suggest a primary functional role for the SFO is sensing circulating apelin.

In conclusion, we have demonstrated two subpopulations of SFO neurons that respond to apelin-13 with depolarization or hyperpolarization. These effects are mediated through the APJ receptor and appear to result from apelin-13-induced activation of NSCCs or potassium channels, respectively. Furthermore, our demonstration that apelin acts directly in SFO to reduce BP and HR suggests the SFO to be a potential CNS site at which circulating apelin acts to influence central cardiovascular control. The present study clearly establishes a unique and pivotal role for SFO in mediating the central effects of apelin.

References

Alim I, Fry WM, Walsh MH & Ferguson AV (2010). Actions of adiponectin on the excitability of subfornical organ neurons are altered by food deprivation. *Brain Res* **1330**, 72–82.

Anthes N, Schmid HA, Hashimoto H, Riediger T & Simon E (1997). Heterogeneous actions of vasopressin on ANG II-sensitive neurons in the subfornical organ of rats. *Am J Physiol* **273**, R2105–R2111.

Azizi M, Iturrioz X, Blanchard A, Peyrard S, De Mota N, Chartrel N, Vaudry H, Corvol P & Llorens-Cortes C (2008). Reciprocal regulation of plasma apelin and vasopressin by osmotic stimuli. *J Am Soc Nephrol* **19**, 1015–1024.

Boucher J, Masri B, Daviaud D, Gesta S, Guigne C, Mazzucotelli A, Castan-Laurell I, Tack I, Knibiehler B, Carpene C, Audigier Y, Saulnier-Blache JS & Valet P (2005). Apelin, a newly identified adipokine up-regulated by insulin and obesity. *Endocrinology* **146**, 1764–1771.

Cayabyab M, Hinuma S, Farzan M, Choe H, Fukusumi S, Kitada C, Nishizawa N, Hosoya M, Nishimura O, Messele T, Pollakis G, Goudsmit J, Fujino M, & Sodroski J (2000). Apelin, the natural ligand of the orphan seven-transmembrane receptor APJ, inhibits human immunodeficiency virus type 1 entry. *J Virol* **74**, 11972–11976.

Cheng X, Cheng XS & Pang CC (2003). Venous dilator effect of apelin, an endogenous peptide ligand for the orphan APJ receptor, in conscious rats. *Eur J Pharmacol* **470**, 171–175.

Collister JP & Nahey DB (2009). The cardiovascular response of normal rats to dual lesion of the subfornical organ and area postrema at rest and to chronic losartan. *Brain Res* **1302**, 118–124.

De Mota N, Reaux-Le GA, El MS, Chartrel N, Roesch D, Dujardin C, Kordon C, Vaudry H, Moos F & Llorens-Cortes C (2004). Apelin, a potent diuretic neuropeptide counteracting vasopressin actions through inhibition of vasopressin neuron activity and vasopressin release. *Proc Natl Acad Sci U S A* **101**, 10464–10469.

Desson SE & Ferguson AV (2003). Interleukin 1β modulates rat subfornical organ neurons as a result of activation of a non-selective cationic conductance. *J Physiol* **550**, 113–122.

El Messari S, Iturrioz X, Fassot C, De Mota N, Roesch D & Llorens-Cortes C (2004). Functional dissociation of apelin receptor signalling and endocytosis: implications for the effects of apelin on arterial blood pressure. *J Neurochem* **90**, 1290–1301.

Ferguson AV, Bicknell RJ, Carew MA & Mason WT (1997). Dissociated adult rat subfornical organ neurons maintain membrane properties and angiotensin responsiveness for up to 6 days. *Neuroendocrinology* **66**, 409–415.

Fry M & Ferguson AV (2009). Ghrelin modulates electrical activity of area postrema neurons. *Am J Physiol Regul Integr Comp Physiol* **296**, R485–R492.

Gruber K, McRae-Degueurce A, Wilkin LD, Mitchell LD & Johnson AK (1987). Forebrain and brainstem afferents to the arcuate nucleus in the rat: potential pathways for the modulation of hypophyseal secretions. *Neurosci Lett* **75**, 1–5.

Habata Y, Fujii R, Hosoya M, Fukusumi S, Kawamata Y, Hinuma S, Kitada C, Nishizawa N, Murosaki S, Kurokawa T, Onda H, Tatemoto K & Fujino M (1999). Apelin, the natural ligand of the orphan receptor APJ, is abundantly secreted in the colostrum. *Biochim Biophys Acta* **1452**, 25–35.

Hindmarch C, Fry M, Yao ST, Smith PM, Murphy D & Ferguson AV (2008). Microarray analysis of the transcriptome of the subfornical organ in the rat: regulation by fluid and food deprivation. *Am J Physiol Regul Integr Comp Physiol* **295**, R1914–R1920.

Hiruma H & Bourque CW (1995). P₂ purinoceptor-mediated depolarization of rat supraoptic neurosecretory cells *in vitro*. *J Physiol* **489**, 805–811.

Horiuchi Y, Fujii T, Kamimura Y, & Kawashima K (2003). The endogenous, immunologically active peptide apelin inhibits lymphocytic cholinergic activity during immunological responses. *J Neuroimmunol* **144**, 46–52.

Hosoya M, Kawamata Y, Fukusumi S, Fujii R, Habata Y, Hinuma S, Kitada C, Honda S, Kurokawa T, Onda H, Nishimura O & Fujino M (2000). Molecular and functional characteristics of APJ. Tissue distribution of mRNA and interaction with the endogenous ligand apelin. *J Biol Chem* **275**, 21061–21067.

Hoyda TD & Ferguson AV (2010). Adiponectin modulates excitability of rat paraventricular nucleus neurons by differential modulation of potassium currents. *Endocrinology* **151**, 3154–3162.

Iturrioz X, Gerbier R, Leroux V, Alvear-Perez R, Maigret B & Llorens-Cortes C (2010). By interacting with the C-terminal Phe of apelin, Phe255 and Trp259 in helix VI of the apelin receptor are critical for internalization. *J Biol Chem* **285**, 32627–32637.

Kagiyama S, Fukuhara M, Matsumura K, Lin Y, Fujii K & Iida M (2005). Central and peripheral cardiovascular actions of apelin in conscious rats. *Regul Pept* **125**, 55–59.

Kawamata Y, Habata Y, Fukusumi S, Hosoya M, Fujii R, Hinuma S, Nishizawa N, Kitada C, Onda H, Nishimura O & Fujino M (2001). Molecular properties of apelin: tissue distribution and receptor binding. *Biochim Biophys Acta* **1538**, 162–171.

Kleinz MJ & Davenport AP (2004). Immunocytochemical localization of the endogenous vasoactive peptide apelin to human vascular and endocardial endothelial cells. *Regul Pept* **118**, 119–125.

Lee DK, Cheng R, Nguyen T, Fan T, Kariyawasam AP, Liu Y, Osmond DH, George SR & O'Dowd BF (2000). Characterization of apelin, the ligand for the APJ receptor. *J Neurochem* **74**, 34–41.

Lee DK, Saldivia VR, Nguyen T, Cheng R, George SR & O'Dowd BF (2005). Modification of the terminal residue of apelin-13 antagonizes its hypotensive action. *Endocrinology* **146**, 231–236.

Lind RW, Van Hoesen GW & Johnson AK (1982). An HRP study of the connections of the subfornical organ of the rat. *J Comp Neurol* **210**, 265–277.

Lv SY, Yang YJ, Qin YJ, Xiong W & Chen Q (2011). Effect of centrally administered apelin-13 on gastric emptying and gastrointestinal transit in mice. *Peptides* **32**, 978–982.

Mangiapane ML & Simpson JB (1980*a*). Subfornical organ lesions reduce the pressor effect of systemic angiotensin II. *Neuroendocrinology* **31**, 380–384.

Mangiapane ML & Simpson JB (1980*b*). Subfornical organ: forebrain site of pressor and dipsogenic action of angiotensin II. *Am J Physiol* **239**, R382–R389.

Medhurst AD, Jennings CA, Robbins MJ, Davis RP, Ellis C, Winborn KY, Lawrie KW, Hervieu G, Riley G, Bolaky JE, Herrity NC, Murdock P & Darker JG (2003). Pharmacological and immunohistochemical characterization of the APJ receptor and its endogenous ligand apelin. *J Neurochem* **84**, 1162–1172.

O'Carroll AM, Selby TL, Palkovits M & Lolait SJ (2000). Distribution of mRNA encoding B78/apj, the rat homologue of the human APJ receptor, and its endogenous ligand apelin in brain and peripheral tissues. *Biochim Biophys Acta* **1492**, 72–80.

Oliet SHR & Bourque CW (1993). Steady-state osmotic modulation of cationic conductance in neurons of rat supraoptic nucleus. *Am J Physiol* **265**, R1475–R1479.

Ono K, Honda E & Inenaga K (2001). Angiotensin II induces inward currents in subfornical organ neurones of rats. *J Neuroendocrinol* **13**, 517–523.

Ono K, Kai A, Honda E & Inenaga K (2008). Hypocretin-1/ orexin-A activates subfornical organ neurons of rats. *Neuroreport* **19**, 69–73.

Paxinos G & Watson C (1982). *The Rat Brain in Stereotaxic Coordinates*. Academic Press, New York.

Price CJ, Rintoul GL, Baimbridge KG & Raymond LA (1999). Inhibition of calcium-dependent NMDA receptor current rundown by calbindin-D28k. *J Neurochem* **72**, 634–642.

Pulman KJ, Fry WM, Cottrell GT & Ferguson AV (2006). The subfornical organ: a central target for circulating feeding signals. *J Neurosci* **26**, 2022–2030.

Reaux A, De Mota N, Skultetyova I, Lenkei Z, El Messari S, Gallatz K, Corvol P, Palkovits M & Llorens-Cortes C (2001). Physiological role of a novel neuropeptide, apelin, and its receptor in the rat brain. *J Neurochem* **77**, 1085–1096.

Reaux A, Gallatz K, Palkovits M & Llorens-Cortes C (2002). Distribution of apelin-synthesizing neurons in the adult rat brain. *Neuroscience* **113**, 653–662.

Riediger T, Rauch M & Schmid HA (1999). Actions of amylin on subfornical organ neurons and on drinking behaviour in rats. *Am J Physiol* **276**, R514–R521.

Roberts EM, Newson MJ, Pope GR, Landgraf R, Lolait SJ & O'Carroll AM (2009). Abnormal fluid homeostasis in apelin receptor knockout mice. *J Endocrinol* **202**, 453–462.

Seyedabadi M, Goodchild AK & Pilowsky PM (2002). Site- specific effects of apelin-13 in the rat medulla oblongata on arterial pressure and respiration. *Auton Neurosci* **101**, 32–38.

Smith PM, Chambers AP, Price CJ, Ho W, Hopf C, Sharkey KA & Ferguson AV (2009). The subfornical organ: a central nervous system site for actions of circulating leptin. *Am J Physiol Regul Integr Comp Physiol* **296**, R512–R520.

Smith PM & Ferguson AV (1997). Vasopressin acts in the subfornical organ to decrease blood pressure. *Neuroendocrinology* **66**, 130–135.

Smith PM & Ferguson AV (2012). Cardiovascular actions of leptin in the subfornical organ are abolished by diet-induced obesity. *J Neuroendocrinol* **24**, 504–510.

Smith PM, Samson WK & Ferguson AV (2007). Cardiovascular actions of orexin-A in the rat subfornical organ. *J Neuroendocrinol* **19**, 7–13.

Sunter D, Hewson AK & Dickson SL (2003). Intracerebroventricular injection of apelin-13 reduces food intake in the rat. *Neurosci Lett* **353**, 1–4.

Taheri S, Zeitzer JM & Mignot E (2002). The role of hypocretins (orexins) in sleep regulation and narcolepsy. *Annu Rev Neurosci* **25**, 283–313.

Takayama K, Iwazaki H, Hirabayashi M, Yakabi K & Ro S (2008). Distribution of c-Fos immunoreactive neurons in the brain after intraperitoneal injection of apelin-12 in Wistar rats. *Neurosci Lett* **431**, 247–250.

Tatemoto K, Hosoya M, Habata Y, Fujii R, Kakegawa T, Zou MX, Kawamata Y, Fukusumi S, Hinuma S, Kitada C, Kurokawa T, Onda H & Fujino M (1998). Isolation and characterization of a novel endogenous peptide ligand for the human APJ receptor. *Biochem Biophys Res Commun* **251**, 471–476.

Tatemoto K, Takayama K, Zou MX, Kumaki I, Zhang W, Kumano K & Fujimiya M (2001). The novel peptide apelin lowers blood pressure via a nitric oxide-dependent mechanism. *Regul Pept* **99**, 87–92.

Tobin VA, Bull PM, Arunachalam S, O'Carroll AM, Ueta Y & Ludwig M (2008). The effects of apelin on the electrical activity of hypothalamic magnocellular vasopressin and oxytocin neurons and somatodendritic peptide release. *Endocrinology* **149**, 6136–6145.

Valle A, Hoggard N, Adams AC, Roca P & Speakman JR (2008). Chronic central administration of apelin-13 over 10 days increases food intake, body weight, locomotor activity and body temperature in C57BL/6 mice. *J Neuroendocrinol* **20**, 79–84.

Washburn DL & Ferguson AV (2001). Selective potentiation of N-type calcium channels by angiotensin II in rat subfornical organ neurones. *J Physiol* **536**, 667–675.

Wei L, Hou X & Tatemoto K (2005). Regulation of apelin mRNA expression by insulin and glucocorticoids in mouse 3T3-L1 adipocytes. *Regul Pept* **132**, 27–32.

Yang B & Ferguson AV (2003). Orexin-A depolarizes nucleus tractus solitarius neurons through effects on nonselective cationic and K^+ conductances. *J Neurophysiol* **89**, 2167–2175.

Zou MX, Liu HY, Haraguchi Y, Soda Y, Tatemoto K & Hoshino H (2000). Apelin peptides block the entry of human immunodeficiency virus (HIV). *FEBS Lett* **473**, 15–18.

Additional information

Competing interests

None.

Author contributions

All experiments were performed in the laboratory of A.V.F. at Queen's University. Patch clamp recording experiments were carried out by L.D. or M.K. while microinjection studies were carried out by P.M.S. All authors were involved in the conception and design of the experiments, the analysis and interpretation of data, and the initial writing and revising of the article in preparation for publication. All authors approved the final version of the manuscript and all persons designated as authors qualify for authorship, and all those who qualify for authorship are listed.

Funding

Acknowledgements